Solving Large Sustainable Supply Chain Networks using Variational Inequalities

Ian Gemp and **Sridhar Mahadevan** and **Bo Liu**
School of Computer Science
University of Massachusetts
Amherst, MA 01003
(imgemp,mahadeva,boliu)@cs.umass.edu

Abstract

In this paper, we explore a new approach to computational sustainability based on variational inequalities (VIs). Our challenge is to compute the steady state behaviors of networks of sustainable supply chains with possibly conflicting objectives. VIs provide a way to model large networks with numerous conflicting goals. Given the size of real-world networks, suitable algorithms must be selected that can scale with the dimension of the problems. In this paper, we explore the effectiveness of novel Runge-Kutta methods on finding equilibrium solutions to two real-world sustainable supply chain problems.

1 Introduction

Businesses and organizations are increasingly modifying their supply chain models to increase sustainability in both their products as well as the processes that act on them. While progress in these areas is still ongoing, improving the network of supply chains remains a challenging problem.

In this paper, we explore a novel approach to computational sustainability in AI, based on the framework of variational inequalities (VIs). Originally proposed by Hartman and Stampacchia (Hartman and Stampacchia 1966) in the context of solving partial differential equations in mechanics, VIs gained popularity in the finite-dimensional setting partly as a result of Dafermos (Dafermos 1980), who showed that the traffic network equilibrium problem could be formulated as a finite-dimensional VI. This advance inspired much follow-on research, showing that a variety of equilibrium problems in economics, game theory, and manufacturing could also be formulated as finite-dimensional VIs – the books by Nagurney (Nagurney 1999; Nagurney and Zhang 1996) and Facchinei and Pang (Facchinei and J. 2003) provide a detailed introduction to the theory and applications.

We apply VIs to the problem of designing sustainable supply chain network models, where the challenging computational problem is to find equilibrium solutions that balance numerous conflicting objectives, covering the cases when problems may or may not have an equivalent convex optimization objective. In the case where a convex optimization formulation does not exist, we are forced to abandon optimization theory and adopt the more general framework of VIs. In the case where such a formulation does exist, the versatility of VIs and the associated algorithm is displayed. In order to solve these vast systems, we will require fast, scalable algorithms suitable to our problems. The primary purpose of this paper is to explain how the theory of VIs provides valuable computational tools for solving large sustainable network systems as well as present a suitable algorithm for solving such systems.

Section 2 describes two real-world supply chains involving a sustainable freightage network and a sustainable blood bank network. Section 3 provides a brief overview of VIs and describes standard algorithms for solving VIs as well as a general Runge-Kutta algorithmic framework that we propose for large domains. In Section 4, we explain the Runge-Kutta (RK) family of methods along with their associated adaptive stepsize scheme. Section 5 compares RK on VI formulations of an emissions conscious freight supply chain network and a perishable goods supply chain. Experiments in both these domains show significant benefits of the proposed RK method.

2 Domain Backgrounds

First, we describe the two sustainable network domains that we'll use in our experiments.

2.1 Sustainable Freightage Network

The Commission for Environmental Cooperation released a report in 2010 focusing on reducing the greenhouse gas (GHG) emissions from freight transportation in North America (ComissionforEnvironmentalCooperation 2010). This report revealed that while "light-duty vehicle GHG emissions are projected...to decline nearly 12%..., Freight trucks, on the other hand, show a projected 20% increase in emissions." Among the commission's key findings is the need for the "greening" of supply-chain management. While some changes to the supply chain like reduced fuel consumption clearly reduce business costs, others may help to mitigate "reputational risk". It's important that the next generation of supply-chain models incorporate these factors in order to reflect the changing goals. The network diagram associated with this problem is shown below in Figure 1,

which is based on a formulation proposed in (Nagurney, Yu, and Floden 2013).

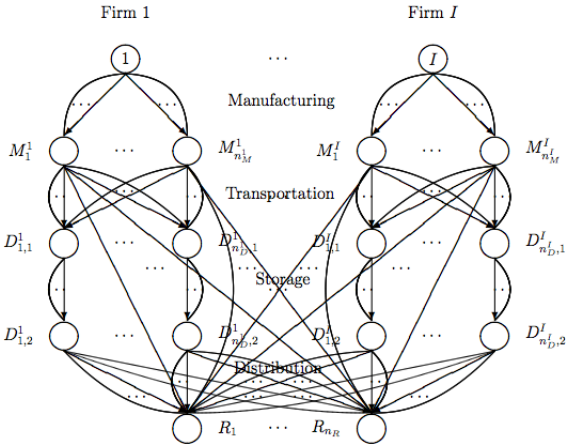

Figure 1: A "green" economic model of the supply chain proposed in (Nagurney, Yu, and Floden 2013). Firms are modeled as playing a Cournot-Nash game, competing on the basis of product flow and frequency of operation. Demand markets consisting of individuals or groups of users choose between the various products offered by the firms.

In this network model, I firms manufacture products which are then either transported directly to retailers (demand markets) or to storage facilities for later distribution. The products in this economy are substitutable and distinguishable only by brand (eg. Oil). In addition, we assume knowledge of the demand functions stating the prices markets are willing to pay for quantities of each product. In Figure 1, the nodes from top tier to bottom tier represent the firms (i), manufacturing plants (M_m^i), storage warehouses ($D_{d,1}^i \& D_{d,2}^i$), and demand markets (R_r). Each link in the network represents a process acting on the product between the origin and destination nodes. From top tier to bottom tier, the links represent manufacturing, transportation, storage, and distribution. Note that each $D_{d,1}^i$ and $D_{d,2}^i$ pair actually represents the same distribution center. This is because storage is a process that starts and ends in the same warehouse, hence the duplication of the nodes.

Each firm must decide how to optimally deliver its product to consumers given the allowable paths from its firm to the multiple demand markets. They do this by controlling their product flows (eg. barrels of oil per day) and frequencies of operation (eg. shipments per day) along paths in the network subject to capacity constraints (eg. barrels per shipment). For example, firm 1 may decide on two paths to optimize its supply chain: each day, two 150-barrel shipments are produced at well 1 and transported using mode 4 (barge) directly to retail market 1 and six 20-barrel shipments are produced at well 1 as well but are then transported using mode 3 (truck) to warehouse 2 for storage until they are finally distributed to retail market 11.

The firms in the network continuously adjust their product flows and operation frequencies, optimizing their utilities, until any unilateral adjustment attempted by one firm is inherently detrimental to that firm's utility function. Rationally competing on the basis of product output is known as Cournot competition and the stalemate described is known as a Nash equilibrium hence this state is known as a Cournot-Nash equilibrium.

Given each firm's utility function and capacity constraints, we aim to find the corresponding steady-state product flows and frequencies of operation.

2.2 Sustainable Blood Banking

Our second example of a sustainable supply chain involves the distribution and supply of blood. According to the American Red Cross, more than 41 thousand blood donations are needed everyday (AmericanRedCross 2014). Extrapolating that number to 365 days implies that there is a need of approximately 15 million blood donations per year. While 15.7 million blood donations are collected each year in the U.S., blood is a perishable product and its collection does not always coincide with its demand, which makes the blood banking system crucial. The blood banking system's effect on sustainability is twofold: one is support for the health of the population by meeting patient demand for blood and the other is the reduction in the amount of medical waste (Nagurney and Masoumi 2012). While the former is a more direct effect, the latter is less obvious. Poor management of medical waste can lead to the contamination of water, soil, and the atmosphere, however, even correct management can be harmful. The ideal method of incineration is one of the top polluters of dioxins and mercury in the US (Giusti 2009). It is important that non-profit organizations such as the American Red Cross be capable of meeting the stochastic demand of patients as closely as possible in order to both support the population and reduce this unnecessary waste. We use the blood supply network shown below in Figure 2, which is based on the formulation proposed in (Nagurney and Masoumi 2012).

In this network model, the organization collects blood at a subset of potential collection sites. Similarly to the freightage model, nodes represent facilities which operate on the blood in some manner and links represent those processes of operation. In this case, the top node, the organization (facility), collects blood (process) at the collection sites (facilities) in the second tier of the network. Following this facility/process paradigm, the blood is then delivered to blood centers (third tier) to be tested, processed (fourth tier), and temporarily stored (fifth tier) after which it is then sent to distribution centers (sixth tier) to ultimately be shipped to demand points (last tier). The demand in these final nodes is assumed to belong to known probability distributions. Also, note the one to one correspondence between the blood centers, component labs, and storage facilities. This is due to the labs and storage facilities often being located within the blood centers, so tiers 3-5 essentially represent the same facility and the links between them are processes that occur within that facility.

The organization must decide how to optimally collect and deliver blood to demand points given the allowable paths. It does this by controlling the blood flow and adjusting process capacities along paths in the network. For example,

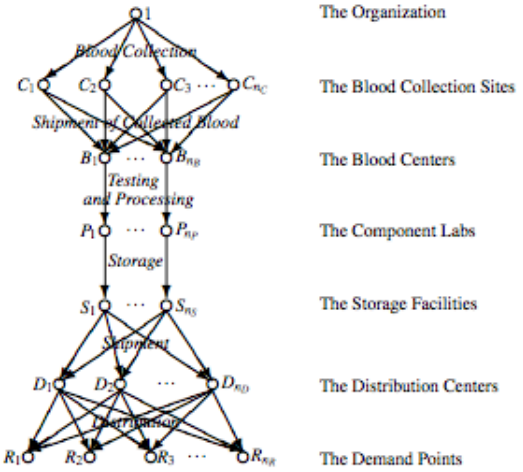

Figure 2: A model of the sustainable blood banking system proposed in (Nagurney and Masoumi 2012). Blood flow and link capacity constraints are adjusted to minimize health and environmental impacts. Individuals or groups of users set demand for blood at the demand points.

the organization may decide to collect 5 liters of blood per day at collection site 1 which it then processes at blood center / component lab / storage facility 2 to be distributed by center 3 to demand point 4. Component lab 2 was originally only equipped to process and test 4 liters of blood per day so the organization incurs an investment cost (eg. more lab equipment) to meet the increased capacity demand. Collection site 1 cannot realistically guarantee the availability of 5 liters of fresh blood each day so there is an associated risk to the organization's expectation that it will have to account for in its utility model. Moreover, any mismatch in supply at the hospitals will result in shortages or surpluses of blood which are costly as well. Furthermore, throughout the supply chain, blood donations expire, test samples are disposed, and surpluses are discarded. For these reasons, each link in the network has a corresponding multiplier representing the fraction of blood that actually survives the process.

In this model, the organization continuously adjusts its blood flows and process capacities in order to minimize all costs (assumed convex) including: operational costs, waste disposal, capacity modification costs, supply shortages/surpluses, and collection risk.

3 Variational Inequalities

The two networks shown in Figure 1 and Figure 2 pose a challenging computational problem, and our proposed solution builds on the mathematical framework of variational inequalities (VIs). As many readers may be unfamiliar with the mathematics of VIs, we begin with a brief review.

3.1 Theory

The formal definition of a VI is as follows:

Definition 1. *The finite-dimensional variational inequality problem VI(F,K) involves finding a vector* $x^* \in K \subset \mathbb{R}^n$ *such that*

$$\langle F(x^*), x - x^* \rangle \geq 0, \ \forall x \in K$$

where $F : K \to \mathbb{R}^n$ *is a given continuous function,* K *is a given closed convex set, and* $\langle ., . \rangle$ *is the standard inner product in* $\mathbb{R}^n$.

Figure 3 provides a geometric interpretation of a variational inequality. The following general result characterizes when solutions to VIs exist:

Theorem 1. *Suppose* K *is compact and that* $F : K \to \mathbb{R}^n$ *is continuous. Then, there exists a solution to VI(*F, K*).*

As Figure 3 shows, x^* is a solution to $VI(F, K)$ if and only if the angle between the vectors $F(x^*)$ and $x - x^*$, for any vector $x \in K$, is less than or equal to 90^0.

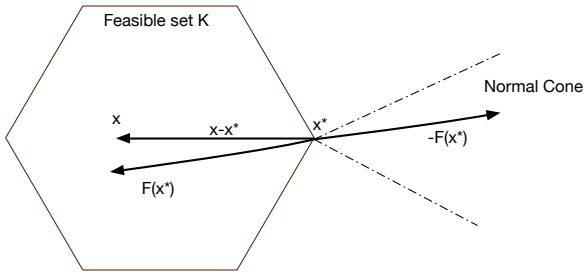

Figure 3: This figure provides a geometric interpretation of the variational inequality $VI(F, K)$. The mapping F defines a vector field over the feasible set K such that at the solution point x^*, the vector field $F(x^*)$ is directed inwards at the boundary, and $-F(x^*)$ is an element of the normal cone $C(x^*)$ of K at x^* where the normal cone $C(x^*)$ at the vector x^* of a convex set K is defined as $C(x^*) = \{y \in \mathbb{R}^n | \langle y, x - x^* \rangle \leq 0, \forall x \in K\}$.

Crucially, VI problems *cannot* be converted back into optimization problems, unless a very restrictive condition is met on the Jacobian of the mapping F.

Theorem 2. *Assume* $F(x)$ *is continuously differentiable on* K *and that the Jacobian matrix* $\nabla F(x)$ *of partial derivatives of* $F_i(x)$ *with respect to (w.r.t) each* x_j *is symmetric and positive semidefinite. Then there exists a real-valued convex function* $f : K \to \mathbb{R}$ *satisfying* $\nabla f(x) = F(x)$ *with* x^**, the solution of VI(F,K), also being the mathematical programming problem of minimizing* $f(x)$ *subject to* $x \in K$.

The algorithmic development of methods for solving VIs begins with noticing their connection to fixed point problems.

Theorem 3. *The vector* x^* *is the solution of VI(F,K) if and only if, for any* $\alpha > 0$*,* x^* *is also a fixed point of the map* $x^* = P_K(x^* - \alpha F(x^*))$*, where* P_K *is the projector onto convex set* K.

In terms of the geometric picture of a VI illustrated in Figure 3, this property means that the solution of a VI occurs at a vector x^* where the vector field $F(x^*)$ induced by F on K

is normal to the boundary of K and directed inwards, so that the projection of $x^* - \alpha F(x^*)$ is the vector x^* itself. This property forms the basis for the projection class of methods that solve for the fixed point.

Definition 2. *A gap function is a function* $\psi : \mathbb{R}^n \to \mathbb{R} \cup \{+\infty\}$ *which satisfies* $\psi(X) \geq 0$ *for all* $X \in K$ *and* $\psi(X^*) = 0, X^* \in K$ *if and only if* X^* *solves* $VI(F, K)$.

Typically, optimization problems are formulated with an objective function, $f(x)$, that may serve as a convergence criterion ($f(x_k) - f(x^*)$), however, a VI formulation does not require an objective function. Gap functions attempt to recover this lost feature. Numerous gap functions have been developed satisfying the properties above (Dutta 2012). One such function, useful in unbounded domains, was developed separately by Fukushima and Auchmuty, $g_\alpha(x)$. We will use $g_2(x)$ later in our experiments to judge convergence.

$$g_\alpha(x) = \sup_{y \in K} \{\langle F(x), x - y\rangle - \frac{\alpha}{2}||x - y||^2\} \qquad (1)$$

3.2 Algorithms

The basic projection-based method (Algorithm 1) for solving VIs is based on Theorem 3 introduced earlier. Here,

Algorithm 1 The Basic Projection Algorithm.

INPUT: Given VI(F,K), and a symmetric positive definite matrix D.

Set $k = 0$ and $x_k \in K$.
repeat
  Set $x_{k+1} \leftarrow P_K(x_k - \alpha D^{-1} F(x_k))$.
  Set $k \leftarrow k + 1$.
until $x_k = P_K(x_k - \alpha D^{-1} F(x_k))$.
Return x_k

P_K is the orthogonal projector onto the convex set K. It can be shown that the basic projection algorithm solves any $VI(F, K)$ for which the mapping F is strongly monotone and Lipschitz smooth. A simple strategy is to set $D = I$ where $\alpha < \frac{L^2}{2\mu}$, L is the Lipschitz smoothness constant, and μ is the strong monotonicity constant. Setting D equal to a constant in this manner recovers what is known as Euler's method and is the most basic algorithm for solving VIs.

The basic projection-based algorithm has two critical limitations. First, it requires that the mapping F be strongly monotone. If, for example, F is the gradient map of a continuously differentiable function, strong monotonicity implies the function must be strongly convex. Second, setting the parameter α requires knowing the Lipschitz smoothness L and the strong monotonicity parameter μ.

The extragradient method of Korpolevich (Korpelevich 1977) addresses some of these concerns, and is defined as Algorithm 2. The extragradient algorithm has been the topic of much attention in optimization since it was proposed, e.g., see (Peng and Yao 2008; Nesterov 2007).

The family of Runge-Kutta (RK) methods induced by Nagurney's general iterative scheme (Nagurney and Zhang 1996) is defined as Algorithm 3. We will explain the motivation behind RK methods in the following section by observing their role in the solution of ordinary differential equations (ODEs). An RK method is defined by its values a and b which are typically presented in what's known as a Butcher table. Heun-Euler and Cash-Karp refer to two tables that we will use in our experiments.

Algorithm 2 The Extragradient Algorithm.

INPUT: Given VI(F,K), and a scalar α.

Set $k = 0$ and $x_k \in K$.
repeat
  Set $y_k \leftarrow P_K(x_k - \alpha F(x_k))$.
  Set $x_{k+1} \leftarrow P_K(x_k - \alpha F(y_k))$.
  Set $k \leftarrow k + 1$.
until $x_k = P_K(x_k - \alpha F(x_k))$.
Return x_k

Algorithm 3 The General Runge-Kutta Algorithm.

INPUT: Given VI(F,K), lower-triangular matrix $a \in \mathbb{R}^{s-1 \times s-1}$, vector $b \in \mathbb{R}^s$, and a sequence of scalars α_k.

Set $k = 0$ and $x_k \in K$.
repeat
  Set $k_1 \leftarrow \alpha_k F(x_k)$
  Set $k_2 \leftarrow \alpha_k F(P_K(x_k - a_{21}k_1))$
  Set $k_3 \leftarrow \alpha_k F(P_K(x_k - a_{31}k_1 - a_{32}k_2))$
  $\vdots$
  Set $k_s \leftarrow \alpha_k F(P_K(x_k - a_{s1}k_1 - \ldots - a_{s,s-1}k_{s-1}))$
  Set $x_{k+1} \leftarrow P_K(x_k - \sum_{i=1}^s b_i k_i)$
  Set $k \leftarrow k + 1$.
until $x_k = P_K(x_k - \sum_{i=1}^s b_i k_i)$.
Return x_k

4 Runge-Kutta Algorithms

In this section, we provide some intuition and explanation for the strengths of Runge-Kutta methods and their associated stepsize scheme.

4.1 The Runge-Kutta Method for ODEs

Runge-Kutta methods are highly popular methods for solving systems of coupled first-order differential equations of the form:

$$\frac{dx}{dt} = f(x, t), \;\; x(t_0) = x_0 \qquad (2)$$

The simplest explicit RK method is Euler's method:

$$x_{k+1} = x_k + \alpha f(x_k, t_k), \;\; t_{k+1} = t_k + \alpha \qquad (3)$$

Euler's method, while simple, is not very accurate because it only uses the derivative of the function at the beginning of the interval. More accurate methods can be designed that advance x_k by a weighted mean of the derivatives of the function in a neighborhood of (x_k, t_k). Runge-Kutta methods are crafted such that the locations and corresponding weights

at which the derivatives are computed induce an approximate taylor series expansion of the algorithm that matches the infinite taylor series expansion of x up to some order p, $\mathcal{O}(h^p)$. The general explicit Runge-Kutta scheme is below where c_i and a_{ij} designate which locations to inspect and b_i defines the weights. Euler's method corresponds to $s = 1, b_1 = 1, c_1 = 1$.

$$x_{k+1} = x_k + \Sigma_{i=1}^{s} b_i k_i, \;\; t_{k+1} = t_k + \alpha, \tag{4}$$

$$k_i = \alpha f(x_k + \Sigma_{j=1}^{i-1} a_{ij} k_j, t_k + c_i \alpha) \tag{5}$$

4.2 Using Adaptive Stepsizes in RK Methods

We now describe an additional enhancement of Runge-Kutta methods that automatically tunes the stepsize. These adaptive methods are designed to produce an estimate of the local truncation error of a single Runge-Kutta step. This can be accomplished by computing and comparing steps with two methods during each iteration of descent, however, more efficient methods make use of the same Runge-Kutta matrix, but differing weights, b_i. This is done by simultaneously using two methods, one with order p and one with order $p-1$. The lower-order step is given by

$$x^*_{k+1} = x_k + \sum_{i=1}^{s} b^*_i k_i, \tag{6}$$

where the k_i are the same as for the higher-order method. Then the error is

$$\Delta_{k+1} = x_{k+1} - x^*_{k+1} = \sum_{i=1}^{s} (b_i - b^*_i) k_i, \tag{7}$$

which is $\mathcal{O}(h^p)$. Stepsizes can be updated as $\alpha_{k+1} \leftarrow \alpha_k \left| \frac{\Delta_0}{\Delta_{k+1}} \right|^{1/p}$, where Δ_0 is the desired accuracy.

Classical gradient rules commonly enforce diminishing stepsizes. The scheme above, however, describes a stepsize that depends on the local behavior of f and may possibly grow with successive iterations. In fact, when used in practice, the stepsize increases as the solution nears the optimum to account for the diminishing value of the gradient.

5 Experiments

We now compare the proposed RK family of methods against standard VI algorithms on the domains discussed in Section 2.

5.1 Sustainable Freightage Network Experiment

Our first example focuses on an emissions-conscious competitive supply chain network (Nagurney, Yu, and Floden 2013). We assume the governing equilibrium is Cournot-Nash and the utility functions are all concave and fully differentiable. This establishes the equivalence between the equilibrium state we are searching for and the variational inequality to be solved where the F mapping is a vector consisting of the negative gradients of the augmented Lagrangian utility functions for each firm. Since F is essentially a concatenation of gradients arising from multiple independent, conflicting objective functions, it does not correspond to the gradient of any single objective function. This forces us to abandon an optimization formulation in favor of a VI formulation.

As this conclusion may trouble some readers, we provide further clarification here. There is no well-behaved objective function whose gradient equates to the F mapping defined in this VI formulation. However, objective functions whose optima directly coincide with the solutions of the VI surely exist, a trivial example being the indicator function to the solutions of the VI ($I^*_X(X)$). It's not clear how one might go about constructing more satisfactory objective functions with the same solutions as the VI. On a more intuitive level, any single utility function that aggregates the interests of all firms cannot act in the interest of all firms simultaneously. As a hypothetical example, imagine the difference between utilities of multiple individual firms competing in a market economy and the utility of a single umbrella corporation in a monopoly; individual voices get lost in this single objective function and the market economy behaves differently.

In the model here, each firm is represented individually. The parameterized utility function for each firm i is presented in Figure 4 and is defined in terms of the product flows (x) on each unique path p from firm i to each of the n_R demand markets k as well as the operation frequencies (γ). Total operational costs, frequency of operation costs, frequency of operation limits, emission costs, demand-price functions, and link-path indicator functions are designated by $\hat{c}$, $\hat{g}$, $\bar{u}$, $\hat{e}$, $\hat{\rho}$, and δ_{ap} respectively. The first three components of the utility function represent profit flow (revenue - operational costs - frequency of operations costs) while the last component represents the costs due to emissions weighted by ω_i.

$U_i = \sum_{l=1}^{n_R} \hat{\rho}_{ik}(x) \sum_{p \in P^i_k} x_p - \sum_{a \in L^i} \hat{c}_a(f) - \sum_{a \in L^i} \hat{g}_a(\gamma_a)$
$-\omega_i \sum_{a \in L^i} \hat{e}_a(f_a, \gamma_a)$
where $x, \gamma \geq 0$ and $f_a = \sum_{p \in P} x_p \delta_{ap} \leq \bar{u}_a \gamma_a, \forall a \in L$

Figure 4: Sustainable Freightage Network Objective Functions

$\langle F(X^*), X - X^* \rangle \geq 0, \forall X \in \mathcal{K},$ where $X = (x, \gamma, \lambda) \in \mathbb{R}^{N_X}_+$
$F^1(X) = \frac{\partial C_p(x)}{\partial x_p} + \omega_i \frac{\partial E_p(x,\gamma)}{\partial x_p} + \sum_{a \in L^i} \lambda_a \delta_{ap} - \rho_{ik}(x)$
$- \sum_{l=1}^{n_R} \frac{\partial \rho_{il}(x)}{\partial x_p} \sum_{q \in P^i_l} x_q; p \in P^i_k; i = 1, \ldots, I; k = 1, \ldots, n_R$
$F^2(X) = \frac{\partial g_a(\gamma_a)}{\partial \gamma_a} + \omega_i \frac{\partial E_p(x,\gamma)}{\partial \gamma_a} - \mu_a \lambda_a; a \in L^i; i = 1, \ldots, I$
$F^3(X) = \mu_a \gamma_a - \sum_{q \in P} x_q \delta_{aq}; a \in L^i; i = 1, \ldots, I$

Figure 5: Sustainable Freightage Network VI

The corresponding variational inequality model presented in Figure 5 is defined with similar terms as above, however, the frequency limits have been folded into the expression through lagrange multipliers (λ) associated with each link a. After some renaming, total operational costs, frequency of operation costs, frequency limits, emission costs, demand-price functions, and link-path indicator functions are designated by C, g, μ, E, ρ, and δ_{ap} respectively. Please see (Nagurney, Yu, and Floden 2013) for more detail.

Figures 6 and 7 reveal the performance gains achieved in employing Runge-Kutta methods, specifically Heun-Euler with $\Delta_0 = 10^{-1}$ (RKHE) and Cash-Karp with $\Delta_0 = 10^{-3}$ (RKCK), over Euler's method and the well-known extragradient (EG) method in determining the solution to the above VI as the size of the network (dimensionality of $X = N_X$) grows. Since in general, the value of our gap function in this example, $g_2(X)$, grows with network size, we elect to judge convergence by the reduction in $g_2(X)$ from the first iteration, $g_2(X)/g_2(X_0) < \epsilon, \epsilon = 10^{-6}$. As you can see from the figures, the Runge-Kutta methods scale better than the other two methods both in terms of number of iterations to convergence and time to completion. Even with constant iterations, runtime increases primarily because the evaluation time of the mapping $F(X)$, F_{eval}, increases by more than 100 times over the growth of the networks.

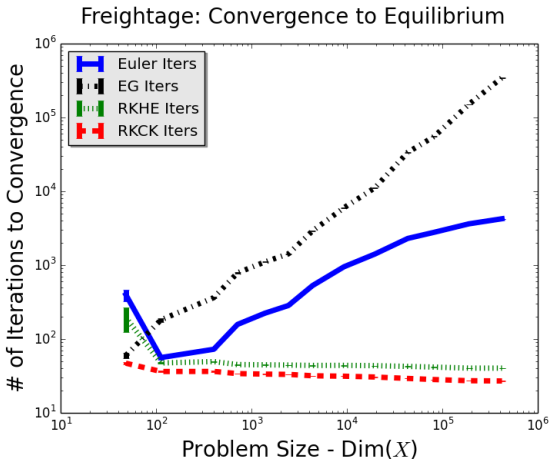

Figure 6: This figure compares our proposed adaptive step-size RK methods against Euler's method (Algorithm 1 where $D = I$) used in (Nagurney, Yu, and Floden 2013) and the well-known extragradient method on the basis of iteration count.

5.2 Sustainable Blood Banking Experiment

In this second experiment, blood donations are accepted at multiple collection sites and transferred through several checkpoints in the supply chain to the demand markets (e.g. hospitals and patients) (Nagurney and Masoumi 2012). In this case, the blood bank supply chain is operated by a single party and so the optimization and variational inequality formulations are equivalent. We use this domain to express VI's flexibility in that regard.

The minimization problem described in Section 2.2 is converted to the variational inequality in Figure 8 by applying Theorem 2. Since the F mapping of the resulting variational inequality is simply the gradient of the Lagrangian formulation for the original objective function, we omit it here. Please see (Nagurney and Masoumi 2012) for more detail.

The corresponding variational inequality model presented in Figure 8 is defined in terms of the blood donation flows

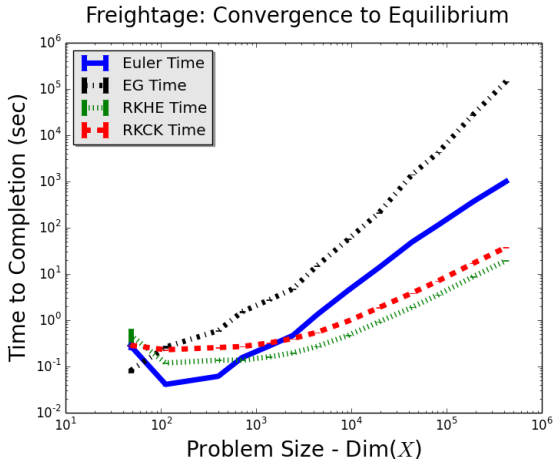

Figure 7: This figure repeats the comparison in Figure 6 on the basis of runtime.

$$\langle F(X^*), X - X^* \rangle \geq 0, \forall X \in \mathcal{K}, \text{ where } X = (x, \mu, \gamma) \in \mathbb{R}_+^{N_X}$$
$$F^1(X) = \frac{\partial(\sum_{q\in\mathcal{P}} \hat{C}_q(x))}{\partial x_p} + \frac{\partial(\sum_{q\in\mathcal{P}} \hat{Z}_q(x))}{\partial x_p}$$
$$+\lambda_k^+ \mu_p P_k\big(\sum_{p\in\mathcal{P}_{w_k}} x_p\mu_p\big) - \lambda_k^- \mu_p\big(1 - P_k\big(\sum_{p\in\mathcal{P}_{w_k}} x_p\mu_p\big)\big)$$
$$+\sum_{a\in L} \gamma_a\delta_{ap} + \theta\frac{\partial(\sum_{q\in\mathcal{P}} \hat{R}_q(x))}{\partial x_p}; p \in P_{w_k}; k = 1, \ldots, n_R$$
$$F^2(X) = \frac{\partial\hat{\pi}_a(u_a)}{\partial u_a} - \gamma_a; a \in L$$
$$F^3(X) = \bar{u}_a + u_a - \sum_{p\in\mathcal{P}} x_p\alpha_{ap}; a \in L$$

Figure 8: Sustainable Blood Banking VI

(x) on each unique path p from the root node to demand market k as well as the capacity adjustments (u) and lagrange multipliers (γ) associated with each link a. The proportion of blood that perishes along each link a and path p in the supply chain is captured by the multipliers α_a and μ_p respectively. Penalties for surpluses and shortages of blood at the demand markets are represented by the third and fourth terms of $F_1(X)$ respectively where P_k is the probability distribution function over the demand for each demand market k. Total operational costs, total discarding costs, and total risk for each path p are designated by $\hat{C}_p$, $\hat{Z}_p$, and $\hat{R}_p$ while total capacity modification cost for each link a is $\hat{\pi}_a$. The constant θ weights the risk, $\hat{R}_p$, associated with blood collection against the other costs mentioned above. The link-path indicator function is denoted by δ_{ap}. The value $\bar{u}_a$ represents the initial flow capacity on link a; in this experiment, we've set all $\bar{u}_a$'s to zero meaning we are building our supply chains from scratch.

Figures 9 and 10 repeat the same ϵ-convergence ($\epsilon = 10^{-3}$) experiment for the blood banking system as Figures 6 and 7 did for the freightage network. Here, RKHE is run with $\Delta_0 = 10^{-5}$ and RKCK with $\Delta_0 = 10^{-6}$. In this case, the Euler and extragradient methods only converge under the iteration limit (10^6) for small scale models. The RK methods, on the other hand, require a scale-free, near constant number of iterations and exhibit much more favorable runtimes. Here, F_{eval} increases by over 1000 times.

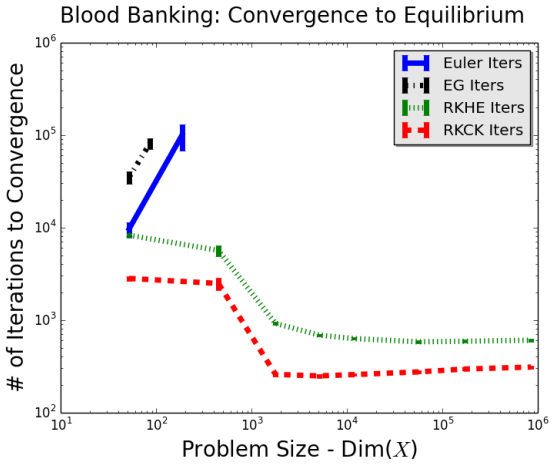

Figure 9: This figure compares our proposed adaptive step-size RK methods against Euler's method (Algorithm 1 where $D = I$) used in (Nagurney and Masoumi 2012) and the well-known extragradient method on the basis of iteration count.

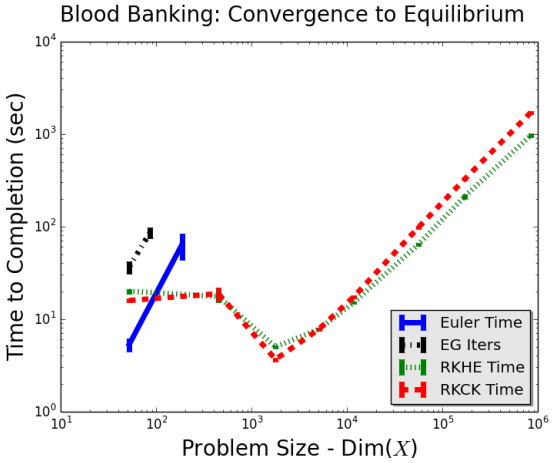

Figure 10: This figure repeats the comparison in Figure 9 on the basis of runtime.

6 Conclusion

In this paper, we proposed a novel computational sustainability framework in AI based on variational inequalities. We analyzed two real-world domains, both involving the transportation of goods across a supply chain network. We proposed a Runge Kutta algorithmic framework to solve such networked VIs, and showed that it scales far better than standard popular algorithms for solving VIs, such as the projection method and the extragradient method. The solutions to these variational inequality formulations contain rich information useful for improving the sustainability of the corresponding networks. For example, emissions regulations would see much less resistance if we could convince businesses that improving their shipping fleets and cutting emissions could result in actual increases in profits. Similarly, equilibrium solutions to the blood bank model would tell us how we could modify existing capacities on links to further minimize our cost function.

References

AmericanRedCross. 2014. Blood facts and statistics. *http://www.redcrossblood.org/learn-about-blood/blood-facts-and-statistics*. Accessed: 2014-08-25.

ComissionforEnvironmentalCooperation. 2010. Destination sustainability: Reducing greenhouse gas emissions from freight transportation in north america. *http://www3.cec.org/islandora/en/item/4237-destination-sustainability-reducing-greenhouse-gas-emissions-from-freight-en.pdf*. Accessed: 2014-08-25.

Dafermos, S. 1980. Traffic equilibria and variational inequalities. *Transportation Science* 14:42–54.

Dutta, J. 2012. When is a gap function good for error bounds? Technical report, Optimization Online.

Facchinei, F., and J., P. 2003. *Finite-Dimensional Variational Inequalities and Complimentarity Problems*. Springer.

Giusti, L. 2009. A review of waste management practices and their impact on human health. *Waste management* 29(8):2227–2239.

Hartman, P., and Stampacchia, G. 1966. On some nonlinear elliptic differential functional equations. *Acta Mathematica* 115:271–310.

Korpelevich, G. 1977. The extragradient method for finding saddle points and other problems. *Matekon* 13:35–49.

Nagurney, A., and Masoumi, A. H. 2012. Supply chain network design of a sustainable blood banking system. In *Sustainable Supply Chains*. Springer. 49–72.

Nagurney, A., and Zhang, D. 1996. *Projected Dynamical Systems and Variational Inequalities with Applications*. Kluwer Academic Press.

Nagurney, A.; Yu, M.; and Floden, J. 2013. Supply chain network sustainability under competition and frequencies of activities from production to distribution. *Computational Management Science* 10(4):397–422.

Nagurney, A. 1999. *Network Economics: A Variational Inequality Approach*. Kluwer Academic Press.

Nesterov, Y. 2007. Dual extrapolation and its application to solving variational inequalities and related problems. *Mathematical Programming Series B.* 109:319–344.

Peng, J., and Yao, J. 2008. A new hybrid extragradient method for generalized mixed equilibrium problems, fixed point problems, and variational inequality problems. *Taiwanese Journal of Mathematics* 12:1401–1432.